

Radiation Sensor Based on MOSFETs Mismatch Amplification for Radiotherapy Applications

Mariano Garcia-Inza, Sebastián H. Carbonetto, José Lipovetzky, and Adrian Faigon

Abstract—In this paper we present a new dosimeter based on a pair of thick gate oxide MOSFET sensors. A differential circuit topology with a feedback loop provides stabilized output with selectable sensitivity amplification for real-time *in vivo* dosimetry. Radiation response shows a wide linear output range and an effective thermal rejection. These properties make this circuit suitable for dose control in radiotherapy applications.

Index Terms—Ionizing Radiation, MOSFET dosimeter, radiotherapy, solid-state detectors.

I. INTRODUCTION

OVER the last years, MOSFET dosimetry in radiotherapy has been thoroughly investigated. Several studies have shown that this type of sensor is suitable for dose control in different radiation therapies [1]–[4]. Dose verification is a key issue, since the efficiency of the treatment relies on a strict accomplishment of the medical planning. This is known as Quality Assurance (QA) in radiation therapy. The International Commission on Radiation Units and Measurements (ICRU) has recommended 5% accuracy in the delivered dose [5]. Considering the complexity of the procedure involved in the delivery of dose to a target volume in a patient, the American Association of Physicists in Medicine (AAPM) requires 3% accuracy in each step dosimetry to achieve the overall 5% along the treatment [6]. Verifying the correct delivery may require the use of portal and verification radiographs, *in vivo* dosimetry, and record-and-verify systems [6].

The use of MOSFETs for *in vivo* dosimetry have several advantages compared to other dosimeters. Their very small size allows very high spatial resolution. For energies in the range of 6–18 MeV they have an excellent performance for surface and dose depth profile [7]. Their radiation response is independent of dose rate. These properties that make them suitable to use with LINAC [8]. As the dosimetric signal is

a voltage, MOSFETs are suitable for integration in electronic systems. Since their response is accumulative with dose they can be read either after or during the exposure to radiation, allowing real-time measurements. Nevertheless some issues have to be taken into account for an accurate dose estimation. MOSFETs usually do not have uniform angular response due to their constructive asymmetry. For photon energies in the range of 0.5–1.25 MeV their response can be energy dependent mainly because of the packaging material [7]. Dose measurement range is limited by the saturation of the sensor which yields a reduction of the sensitivity [9]. Moreover, temperature drifts affect the dosimetric signal and can cause an erroneous dose measurement [10].

Temperature and measurement range limitations of the MOSFET dosimeter are addressed in this work. During *in vivo* dosimetry temperature variations in the sensor can occur when it is placed in contact with the patient's body. This produces a shift from room to body temperature that should be taken into account when reading the dosimeter. In case of *real-time* measurements one option is to track the sensor's temperature and wait for it to stabilize before the exposure. This will avoid the drift of the dosimetric signal that introduces an error in the dose estimation, but implies a significant time loss in the treatment. Another approach is to read the MOSFET sensor using the minimum temperature coefficient (MTC) current [10]. The drawback in this case is that the value of I_{MTC} depends on the accumulated dose [11], so the sensor has to be recalibrated periodically to assure the accuracy of the dose estimation.

In this paper we propose a differential sensor topology which provides thermal drift rejection, sensitivity amplification, and extended measurement range. Dose estimation using a pair of MOSFETs was initially proposed in [12]. Recently we have explored the use of differential biasing technique showing its performance in real-time measurements [13]. Next we proposed a differential circuit with amplification [14] obtaining much higher sensitivity than the former one, but the circuit showed limitations in the linear range and in the temperature response. In this paper we present a new differential dosimeter that amplifies the mismatch between a pair of MOSFET sensors. A feedback loop allows to fix the sensitivity gain to a known value providing a stabilized response with a larger linear output.

The aim of this work is to evaluate the radiation response of a new dosimeter circuit topology for future monolithic integration. Several groups have investigated and presented promising results of ASICs for dosimetry using floating-gate devices as radiation sensors: [15]–[18]. Our investigation is

Manuscript received December 3, 2015; revised March 7, 2016; accepted April 25, 2016. Date of publication May 3, 2016; date of current version June 21, 2016. This work was supported by the ANPCyT and UBA by the grants PICT Redes 2007–1907 and UBACyT Q025.

M. Garcia-Inza and A. Faigon are with the Device Physics-Microelectronics Laboratory, INTECIN, Facultad de Ingeniería, Universidad de Buenos Aires, Ciudad Autónoma de Buenos Aires, Argentina, and also with the National Scientific and Technical Research Council of Argentina (CONICET) (e-mail: mgarciaianza@fi.uba.ar).

S. Carbonetto is with the Device Physics-Microelectronics Laboratory, INTECIN, Facultad de Ingeniería, Universidad de Buenos Aires, Ciudad Autónoma de Buenos Aires, Argentina (e-mail: scarbonetto@fi.uba.ar).

J. Lipovetzky is with the Centro Atómico Bariloche Comisión Nacional de Energía Atómica (CAB-CNEA), Pcia. de Río Negro, Argentina, and also with the National Scientific and Technical Research Council of Argentina (CONICET), Argentina.

Color versions of one or more of the figures in this paper are available online at <http://ieeexplore.ieee.org>.

Digital Object Identifier 10.1109/TNS.2016.2560172

focused on differential circuits with thick gate oxide MOSFET sensors to develop a system-on-chip dosimeter for radiotherapy applications.

The paper has the following organization. Section II gives a full description of the dosimeter, i.e., the MOSFET sensors, the biasing technique, the reading circuit, and its implementation. In Section III we describe the measurement setup and their results. Section IV presents the discussion and conclusions.

II. SENSOR DESCRIPTION

A. Working Principle

The dosimeter is based on a pair of MOSFETs fabricated with thick gate oxide for improved sensitivity. This sensing pair was pre-irradiated to lower their threshold voltage (V_T). Then, a differential biasing technique is applied [13]. During exposure one device is biased with positive gate voltage, which contributes to the *positive charge build-up* (PCB) within the gate oxide, reducing V_T [19], whereas the other MOSFET is biased with negative voltage. This produces a phenomenon called *radiation-induced charge neutralization* (RICN), which recovers V_T [20]. These effects occurring simultaneously affect both devices differently, forcing their mismatch. The threshold voltage offset can be taken as the dosimetric signal. Periodically, the devices have to be commuted from biasing to reading configuration in order to measure the induced mismatch.

The V_T s of the MOSFETs can be kept within a measurable range by switching the gate biasing voltage between a positive and a negative value for PCB and RICN respectively. This procedure, named *bias cycled controlled measurement* (BCCM) was initially proposed in [21] and applied to other dosimeters in [22] and [23]. Later, a differential version was developed and presented in [13]. The technique allows to extend the measurement range of the dosimeter, since the V_T of the devices are kept between a maximum and a minimum value avoiding the response saturation regions.

B. Dosimeter Circuit Description

Fig. 1 shows the circuit configurations of the dosimeter. $M1$ and $M2$ are thick gate oxide MOSFETs built in the same silicon chip. Fig. 1(a) shows the biasing mode in which independent gate voltages are applied to each device. Solid-state switches allow to periodically commute the dosimeter to reading mode of Fig. 1(b). In this configuration V_{GS1} is fixed by the voltage source V_{REF} which defines the drain current I_{D1} . The resistor R_{D1} determines the drain voltage of $M1$. The operational amplifier (OA) sets its output to force the same voltage in the drain of $M2$. Choosing $R_{D2} = R_{D1}$ results in the same current for both MOSFETs; thus the voltage difference between their gates can be taken as the offset of the pair: $V_{OFF} = V_{G2} - V_{G1}$. The feedback resistors R_{f1} and R_{f2} set the offset amplification. The expression of V_{OUT} is

$$V_{OUT} = V_{REF} + V_{OFF} \left(1 + \frac{R_{f1}}{R_{f2}} \right). \quad (1)$$

The circuit allows to amplify the offset voltage of the MOSFET sensing pair. The differential nature of V_{OFF} rejects

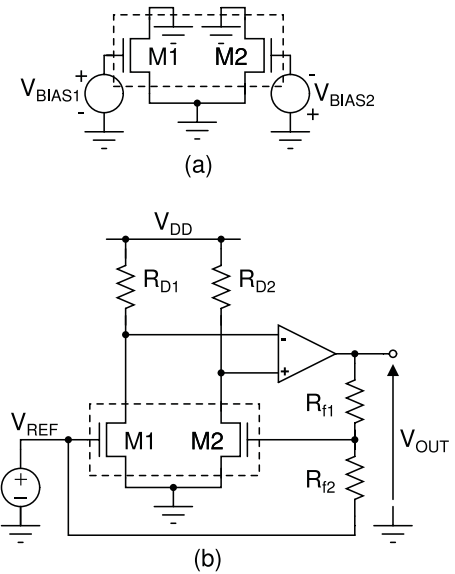


Fig. 1. Dosimeter circuit in (a) biasing and (b) reading modes. To commute, solid-state switches (not shown) are used. Devices in the dashed box comprise the sensing pair fabricated in the same silicon chip.

common mode perturbations as thermal drifts or variations in V_{DD} . V_{OUT} is an amplified single-output copy of V_{OFF} . The selection of R_{f1} and R_{f2} defines the feedback loop and fixes the amplification gain.

C. Circuit Implementation

The thick gate oxide MOSFETs used as radiation sensors in this work are field oxide field effect transistors (FOXFETs). A detailed description of them can be found in [24]. These devices were fabricated in a CMOS technology and integrated in the same silicon chip. The gate oxide thickness of the FOXFET is ≈ 590 nm, exhibiting a response of 4.2 mV/rad(SiO_2) with gate bias of 10 V. Since the threshold voltage of the fresh samples is 28 V, the devices were preirradiated to lower V_T down to 7 V.

Solid-state switches MAX4533 were used to commute the circuit between biasing and reading modes. The OA was an OP07; drain resistors value were 47 k Ω , and the feedback resistors were selectable through jumpers or a trimpot. The circuit was implemented in two different boards. One with the FOXFET pair and a thermistor, and the other board with the remaining components. The FOXFETs were encapsulated in a DIP40 ceramic package, and both boards were connected by flat cable (7 \times 40 cm). Separated boards allow to irradiate the FOXFET sensing pair while keeping the other components of the circuit away from the radiation field.

The power supply used was external with $V_{DD} = 18$ V and $V_{REF} = 9$ V.

III. MEASUREMENTS

A. Setup Description

The sensors' board containing a pair of FOXFETs was irradiated in an INVAP TERADI 800 ^{60}Co teletherapy system. Fig. 2 shows a schematic of the experimental setup. The sensors' board was placed on the stretcher and exposed to

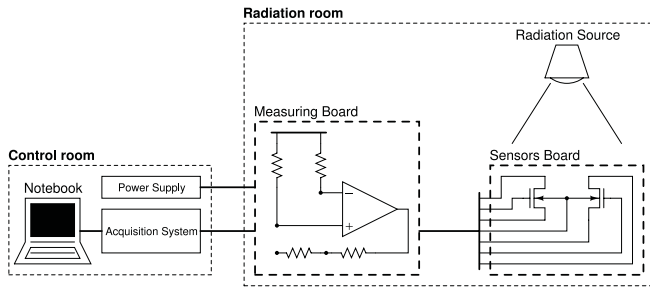


Fig. 2. Experimental setup.

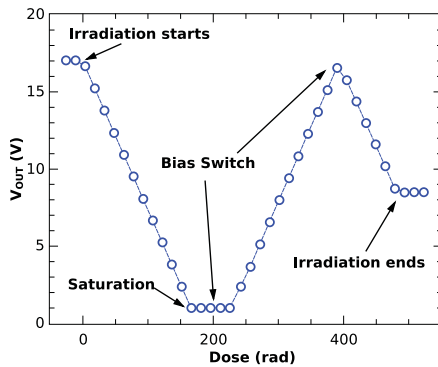


Fig. 3. Gamma radiation response of the circuit with gain 17x.

the gamma source with a field size of 15 cm \times 15 cm at a distance of 80 cm obtaining a dose rate of 75 rad(SiO₂)/min.

The measuring board which contains the components for biasing and reading the sensors was placed on the stretcher outside the radiation field.

The acquisition system used was a portable Agilent 34970A commanded with a notebook both located in the control room. A 10-m-long multipair cable with shield was used to connect to the dosimeter's circuit. The measured signals were V_{OUT} , V_{RD1} (the voltage drop in resistor R_{D1}), and V_{OFF} . The sensor temperature (TEMP) was also recorded using a thermistor in contact with the FOXFETs package.

The Agilent unit generated the digital signal to commute the dosimeter between biasing and reading mode. It also provided the gate bias voltages: 10 V for PCB and -10 V for RICN. The sampling period was 11 s.

B. Output Linear Range

The proposed dosimeter was initially irradiated to explore the output range and the linearity of the response. The feedback resistors were set to obtain a 17x gain. Fig. 3 shows the time evolution of the output voltage. When the exposure starts the output evolves toward lower values due to the proper biasing of each FOXFET. For $V_{OUT} \approx 1$ V the reading circuit saturates. Then the FOXFETs bias was switched and V_{OUT} changed its slope, starting to recover. For an accumulated dose of 389 rad(SiO₂) the biasing voltages are switched again to change the slope in the evolution of V_{OUT} . This response showed that the circuit is suitable to operate under the BCCM technique.

The linear region of V_{OUT} showed in Fig. 3 extends from 1 to 17 V. Within this range V_{OUT} adjusts to a linear response

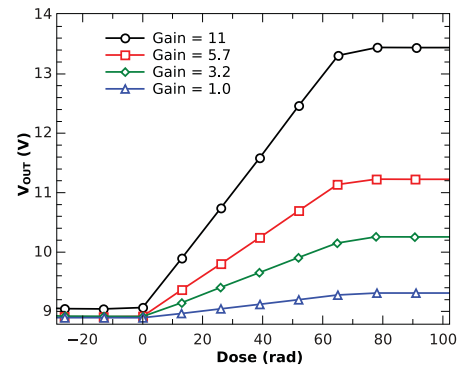


Fig. 4. Circuit response to 60 s gamma pulses with different gain configurations for positive slope response.

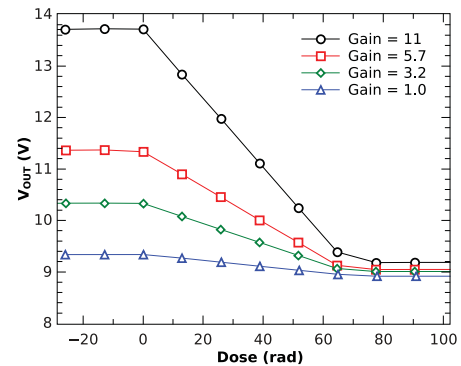


Fig. 5. Circuit response to 60 s gamma pulses with different gain configurations for negative slope response.

with $R^2 = 0.9998$. The effective sensitivity is 95.5 mV/rad with a difference lower than 0.2% between positive and negative slopes.

C. Different Gains for a Fixed Gamma Dose

Next, the system was tested with gamma pulses of 60 s length to emulate a radiotherapy procedure. The radiation pulses were repeated for positive and negative slopes with different gain configurations. The measurement sequence was the following: i) resistors gain setting; ii) 60 s exposure; iii) bias switch; and iv) 60 s exposure. Gains used were: 1.0, 3.2, 5.7, and 11.0x. The results are shown in Figs. 4 and 5. In the first, measurements with different gains and positive slope response are plotted together against each relative dose. The second one gathers negative slope measurements.

For gain 1.0x, the traces V_{OUT} of Figs. 4 and 5 are V_{OFF} . In this case the sensitivity obtained was 5.6 mV/rad(SiO₂) which can be considered the intrinsic response of the sensor. For the other measured gains the obtained sensitivity were: 17.9, 31.9, and 61.6 mV/rad(SiO₂).

D. Temperature Coefficient

Fig. 6 shows the result of applying a slow thermal sweep to the dosimeter (gain 1.0x) without the presence of radiation field. The temperature coefficient estimated from the shift induced in V_{OUT} was 0.4 mV/°C.

The ratio between the intrinsic radiation response and the temperature coefficient is the *temperature error*

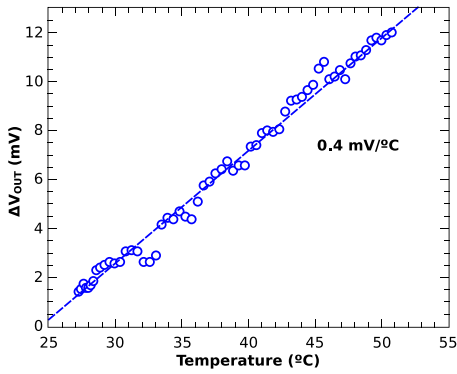


Fig. 6. Temperature circuit response.

factor (TEF) [13]. This figure of merit gives the absolute error in the dose measurement per unit of temperature change during the irradiation. In this case $TEF = 71 \text{ mrad}(\text{SiO}_2)/^\circ\text{C}$.

It is important to notice that TEF does not depend on the gain configuration, since both the temperature coefficient and the radiation sensitivity are amplified by the reading circuit.

E. BCCM Operation Under Temperature Perturbation

In a new experiment, the differential BCCM technique was applied for a long continuous radiation exposure. During it a temperature perturbation was induced externally. This allows to evaluate the thermal rejection along the irradiation.

For this test a hot air gun was also placed on the stretcher of the radiotherapy unit pointing to the sensors board. Special care was taken to avoid affecting the reading circuit (measuring board). The ON-OFF swch was in the control room allowing to start and stop the gun without interrupting the irradiation.

The feedback resistors were set using the configurable trimpot. The measurement range was extended by switching the biasing voltages of the FOXFETs alternating positive slope stages with negative slope stages. The BCCM technique was programmed to keep V_{OUT} within a window limited by 10 V and 8 V (this is $V_{REF} \pm 1 \text{ V}$).

The evolution of the signals along the test are shown in Fig. 7 (V_{RD1} , TEMP) and Fig. 8 (V_{OUT}). The temperature perturbation started when the accumulated dose was 245 rad(SiO_2). The hot air gun was switched ON for 25 s rising the temperature of the FOXFETs from 25 °C to 90 °C measured at the packaging surface. When the hot air is switched OFF temperature falls slowly to room temperature. Fig. 8 and its derivative (Fig. 9) show the robustness against temperature of the BCCM signal output compared with the single-sensor output shown in Fig. 7.

Fig. 9 shows the instant radiation sensitivity of V_{OUT} which was $27.3 \pm 0.8 \text{ mV/rad}(\text{SiO}_2)$. The mean and standard deviation did not change along the test showing the ability of the BCCM technique to extend the useful dosimeter range.

F. Noise

The electrical noise of V_{OUT} was estimated for different gains in absence of the radiation field. With this purpose

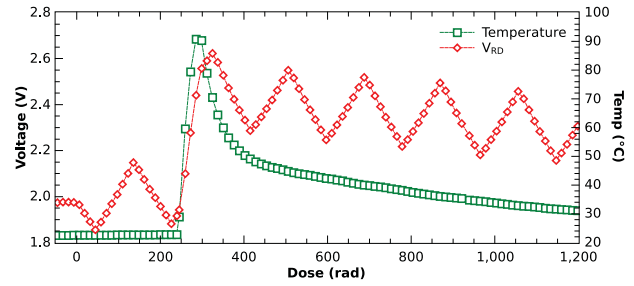


Fig. 7. Temperature of the sensor package and voltage drop in R_{D1} .

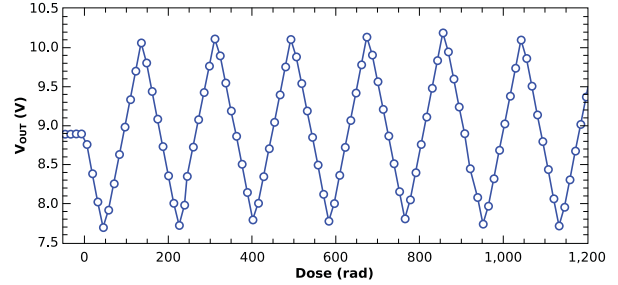


Fig. 8. V_{OUT} during a extended irradiation with a temperature perturbation.

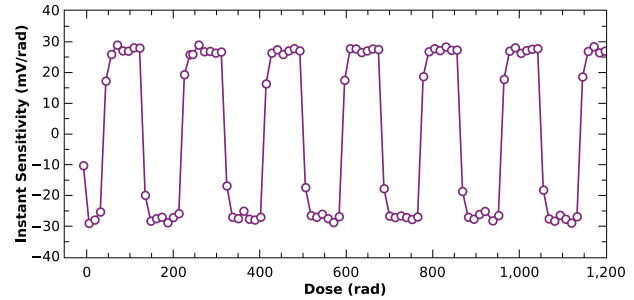


Fig. 9. Instant sensitivity of V_{OUT} along the irradiation with temperature perturbation.

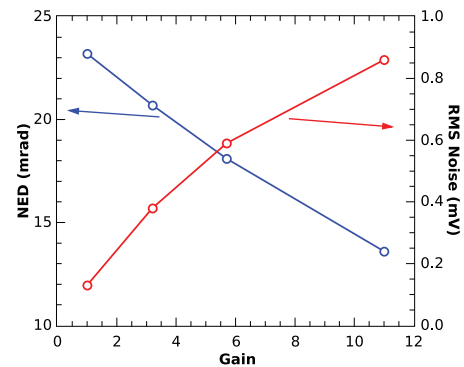


Fig. 10. RMS noise level of V_{OUT} for different gains.

2-hour-long measurements were processed to obtain the RMS value of the electrical signal.

Fig. 10 shows that noise increases with gain. For gain 1x the noise level is 0.13 mV_{RMS} , and for 11x it is 0.86 mV_{RMS} , showing that the noise increment is not proportional to the sensitivity gain.

TABLE I

COMPARISON BETWEEN THE DOSIMETERS: SINGLE MOSFET, FULLY DIFFERENTIAL CIRCUIT, AND THE MISMATCH AMPLIFIED DOSIMETERS. TEMPERATURE ERROR FACTOR, NOISE-EQUIVALENT DOSE, AND RADIATION SENSITIVITY (DOSES ARE REFERRED TO SiO_2). ALL THE RESULTS OF THIS USING FOXFETs OF [24] AS THE RADIATION SENSORS.

Dosimeter	TEF ($\text{mrad}/^\circ\text{C}$)	NED (mrad)	S_R (mV/rad)
Single MOSFET [24]	586	12	4.2
Fully Differential [13]	27	20	4.8 ^(c)
Mismatch Amp.	71	14 ^(a)	5.6 ^(b)

(a) Gain 11.0x. (b) Gain 1.0x (intrinsic sensitivity).
(c) with different biasing conditions than in case (b).

The *noise-equivalent dose* (NED) [13] calculated as the ratio between RMS noise level and radiation sensitivity is plotted in the same figure. Its reduction with gain, from 23 $\text{mrad}(\text{SiO}_2)$ for gain 1x to 14 $\text{mrad}(\text{SiO}_2)$ for 11x, is the result of a higher increase in the sensitivity than in the noise level.

This result can be explained considering that noise has two components: one from the sensors (inherent flicker noise of the MOS structure), and other from the board that includes the components of the circuit and the connection cables. The first component is amplified by the reading circuit, but the second remains constant. Thus, the total noise level in V_{OUT} increases less than the amplification.

IV. DISCUSSION AND CONCLUSION

The reading circuit proposed in this paper showed an amplified and stable linear radiation response. This is due to the feedback loop that allows to set the sensitivity gain by selecting the value of the resistors R_{f1} and R_{f2} . The dosimeter was tested under gamma radiation of ^{60}Co with several gain values. The thermal response of the dosimeter was characterized obtaining a temperature coefficient of $0.4 \text{ mV}/^\circ\text{C}$. The differential topology showed to be effective to mitigate temperature drifts during the radiation tests. These properties make this prototype suitable for *in vivo-real-time* radiotherapy applications.

Experimental results show that the sensor can be used for short pulses of radiation and also for long continuous exposures. This was achieved by applying the differential BCCM technique that allows to extend the measurement range of the MOS sensors. A total dose of 4 $\text{krad}(\text{SiO}_2)$ was measured without sensitivity loss.

Table I summarizes the results obtained with the Mismatch Amplifier dosimeter presented in this paper and compares them with previous works.

The *temperature error factor* achieved with the amplified circuit is more than eight times lower than the Single MOSFET dosimeter. This shows the advantages of the differential topology. Even though, the Mismatch Amplifier presented higher TEF than the Fully Differential [13] version (71 against 27 $\text{mrad}(\text{SiO}_2)$). This better performance of the Fully Differential dosimeter can be attributed to the symmetry of its topology as both branches of the circuit are identical. The Mismatch Amplifier design lacks of this property, since the gate of $M1$ is connected to a voltage reference and the gate of $M2$ is set by the feedback loop.

The *noise-equivalent dose* estimated for the dosimeter presented in this paper was 14 $\text{mrad}(\text{SiO}_2)$ when the gain is 11.0x. This value is achieved thanks to the sensitivity amplification, as can be seen in Fig. 10. The Fully Differential dosimeter which is not amplified has a NED of 20 $\text{mrad}(\text{SiO}_2)$. This reduction in the NED is a benefit of the amplified topology and the fewer components of the circuit. The Single MOSFET is the simplest dosimeter and reaches the lowest value with 12 $\text{mrad}(\text{SiO}_2)$.

The intrinsic radiation sensitivity (S_R) for the proposed dosimeter was measured obtaining 5.6 $\text{mV}/\text{rad}(\text{SiO}_2)$. Several amplifications were also tested obtaining sensitivities up to 95.5 $\text{mV}/\text{rad}(\text{SiO}_2)$. The Fully Differential sensor has a response of 4.8 $\text{mV}/\text{rad}(\text{SiO}_2)$, but under different biasing conditions. The Single MOSFET dosimeter used in the standard procedure has lower sensitivity (4.2 $\text{mV}/\text{rad}(\text{SiO}_2)$) than both differential dosimeters. This is because its response depends only in PCB within the oxide, while in the differential topologies it depends on the difference between PCB and RICN of each device.

The resolution of the proposed dosimeter can be estimated considering the noise performance of the output. In a thermal stabilized scenario, the minimum detectable dose can be calculated as four times the NED [25] resulting in 56 $\text{mrad}(\text{SiO}_2)$.

Based on the satisfactory results obtained with the proposed circuit, future work will be aimed to integrate the circuits of Fig. 1 together with the FOXFET pair, the switches, and its control logic in the same silicon chip. This approach is feasible, since all the devices involved in the dosimeter can be fabricated in a standard CMOS technology. Being the gate oxide of the FOXFETs 40 times thicker than the native MOSFETs of the process, it is expected that the radiation response will be dominated by FOXFETs devices. The integrated system design has several challenges, such as the radiation hardening of the reading and control circuits, and the high-voltage operation. Direct advantages of a system-on-chip dosimeter would be as follows.

- It eliminates the reading circuit board making the dosimeter much smaller and easier to use for *in vivo* applications.
- The noise of the sensor will be reduced since the FOXFET pair can be amplified in situ. This implies an improvement in its dose resolution.
- Selectable gain can increase signal-to-noise ratio when measuring low doses in real-time measurements.

The high sensitivity and extended measurement range enable this dosimeter to be used in dose control in radiotherapy, radiology, or computed tomography. Due to its small size and its easy reading mode, it could be directly integrated in the medical equipment, mounted on a catheter for intracavitary measurements, or could be used in a spatial array for field profile verification.

ACKNOWLEDGMENT

The authors would like to thank Marie Curie Hospital (Buenos Aires city, Argentina) for the access to irradiation facilities.

REFERENCES

- [1] M. Dybek, W. Lobodziec, A. Kawa-Iwanicka, and T. Iwanicki, "MOSFET detectors as a tool for the verification of therapeutic doses of electron beams in radiotherapy," *Rep. Pract. Oncol. Radiother.*, vol. 10, no. 6, pp. 301–306, 2005.
- [2] N. Hardcastle, D. Cutajar, P. Metcalfe, M. Lerch, V. Perevertaylo, W. Tome, and A. Rosenfeld, "In vivo real-time rectal wall dosimetry for prostate radiotherapy," *Phys. Med. Biol.*, vol. 55, no. 13, pp. 3859–3871, 2010.
- [3] K. Y. Quach, J. Morales, M. J. Butson, A. B. Rosenfeld, and P. E. Metcalfe, "Measurements of radiotherapy X-ray skin dose on a chest wall phantom," *Med. Phys.*, vol. 27, no. 7, pp. 1676–1680, 2000.
- [4] A. Ismail, J. Giraud, G. Lu, R. Sihanath, P. Pittet, J. Galvan, and J. Balosso, "Radiotherapy quality insurance by individualized in vivo dosimetry: State of the art," *Cancer/Radiothrapie*, vol. 13, pp. 182–189, 2009.
- [5] Int. Commiss. on Radiation Units and Measurement (ICRU), Determination of Absorbed Dose in a Patient Irradiated by Beams of X- or Gamma-Rays in Radiotherapy Procedures, IRep. 24, 1976.
- [6] AAPM, Comprehensive QA for Radiation Oncology Amer. Assoc. Phys. Med., Alexandria, VA, USA, Rep. 46.
- [7] A. B. Rosenfeld, M. G. Carolan, G. I. Kaplan, B. J. Allen, and V. I. Khivrich, "MOSFET dosimeters: the role of encapsulation on dosimetric characteristics in mixed gamma-neutron and megavoltage X-ray fields," *IEEE Trans. Nucl. Sci.*, vol. 42, no. 6, pp. 1870–1877, Dec. 1995.
- [8] A. B. Rosenfeld, "MOSFET dosimetry on modern radiation oncology modalities," *Rad. Prot. Dos.*, vol. 101, nos. 1–4, pp. 393–398, 2002.
- [9] H. E. Boesch, F. B. McLean, J. M. Benedetto, J. M. McGarrity, and W. E. Bailey, "Saturation of threshold voltage shift in MOSFET's at high total dose," *IEEE Trans. Nucl. Sci.*, vol. 33, no. 6, pp. 1191–1197, Eec. 1986.
- [10] G. Sarrabayrouse and S. Siskos, "Temperature effects and accuracy of MOS radiation dosimeters," in *Proc. 7th WSEAS Int. Conf. Microelectronics, Nanoelectronics, Optoelectronics*, 2008, pp. 26–30.
- [11] S. H. Carbonetto, M. Garcia-Inza, J. Lipovetzky, E. G. Redin, L. Salomone, and A. Faigon, "Zero temperature coefficient bias in MOS devices. Dependence on interface traps density, application to MOS dosimetry," *IEEE Trans. Nucl. Sci.*, vol. 58, no. 6, pp. 3348–3353, Dec. 2011.
- [12] M. Soubra, J. Cygler, and G. Mackay, "Evaluation of a dual bias dual metal oxide-silicon semiconductor field effect transistor detector as radiation dosimeter," *Med. Phys.*, vol. 21, no. 4, pp. 567–572, 1994.
- [13] M. Garcia-Inza, S. Carbonetto, J. Lipovetzky, M. Carra, L. S. Salomone, E. Redin, and A. Faigon, "Switched bias differential MOSFET dosimeter," *IEEE Trans. Nucl. Sci.*, vol. 61, no. 3, pp. 1407–1413, Jun. 2014.
- [14] S. Carbonetto, M. Garcia-Inza, J. Lipovetzky, M. Carra, E. Redin, L. S. Salomone, and A. Faigon, "CMOS differential and amplified dosimeter with field oxide n-channel MOSFETs," *IEEE Trans. Nucl. Sci.*, vol. 61, no. 6, pp. 3466–3471, Dec. 2014.
- [15] E. Garcia-Moreno, E. Isern, M. Roca, R. Picos, J. Font, J. Cesari, and A. Pineda, "Temperature compensated floating gate MOS radiation sensor with current output," *IEEE Trans. Nucl. Sci.*, vol. 60, no. 5, pp. 4026–4030, Oct. 2013.
- [16] E. G. Villani, A. Gabrielli, A. Khan, E. Pikhay, Y. Roizin, and Z. Zhang, "Monolithic 180 nm CMOS dosimeter for in vivo medical applications," *IEEE Trans. Nucl. Sci.*, vol. 60, no. 2, pp. 843–849, Apr. 2013.
- [17] M. Arsalan, A. Shamim, M. Shams, N. G. Tarr, and L. Roy, "Ultra low power CMOS-based sensor for on-body radiation dose measurements," *IEEE J. Emerging Sel. Topics Circuits Syst.*, vol. 2, no. 1, pp. 34–41, Mar. 2012.
- [18] M. Alvarez, C. Hernando, J. Cesari, A. Pineda, and E. Garcia-Moreno, "Total ionizing dose characterization of a prototype floating gate MOSFET dosimeter for space applications," *IEEE Trans. Nucl. Sci.*, vol. 60, no. 6, pp. 4281–4288, Dec. 2013.
- [19] J. R. Schwank, M. R. Shaneyfelt, D. M. Fleetwood, J. A. Felix, P. E. Dodd, P. Paillet, and V. Ferlet-Cavrois, "Radiation effects in MOS oxides," *IEEE Trans. Nucl. Sci.*, vol. 55, no. 4, pp. 1833–1853, Aug. 2008.
- [20] D. M. Fleetwood, "Radiation induced charge neutralization and interface trap buildup in metal oxide semiconductor devices," *J. Appl. Phys.*, vol. 67, no. 1, pp. 580–583, 1990.
- [21] A. Faigon, J. Lipovetzky, E. Redin, and G. Krusczenski, "Extension of the measurement range of MOS dosimeters using radiation induced charge neutralization," *IEEE Trans. Nucl. Sci.*, vol. 55, no. 4, pp. 2141–2147, Aug. 2008.
- [22] M. Garcia Inza, J. Lipovetzky, E. G. Redin, S. Carbonetto, and A. Faigon, "Floating gate PMOS dosimeters under bias controlled cycled measurement," *IEEE Trans. Nucl. Sci.*, vol. 58, no. 3, pp. 808–812, Jun. 2011.
- [23] J. Lipovetzky, A. Siedle, M. Garcia-Inza, S. Carbonetto, E. Redin, and A. Faigon, "New fowler-nordheim injection, charge neutralization, and gamma tests on the REM RFT300 RADFET dosimeter," *IEEE Trans. Nucl. Sci.*, vol. 59, no. 6, pp. 3133–3140, Dec. 2012.
- [24] J. Lipovetzky, M. Garcia-Inza, S. Carbonetto, M. J. Carra, E. G. Redin, L. S. Salomone, and A. Faigon, "Field oxide n-channel MOS dosimeters fabricated in CMOS processes," *IEEE Trans. Nucl. Sci.*, vol. 60, no. 6, pp. 4683–4691, Dec. 2013.
- [25] N. Tarr, C. Plett, A. Yeaton, G. Mackay, and I. Thomson, "Limitations on MOSFET dosimeter resolution imposed by 1/f noise," *IEEE Trans. Nucl. Sci.*, vol. 43, no. 5, pp. 2492–2495, Oct. 1996.